Paper 312

Proceedings of the Second International Conference on Railway Technology: Research, Development and Maintenance, J. Pombo, (Editor),
Civil-Comp Press, Stirlingshire, Scotland.

Elimination of Failures in Railway Gearboxes by Regenerative Coasting

A. Bracciali and F. Piccioli
Dipartimento di Ingegneria Industriale
Università di Firenze, Italy

Abstract

Railway gearboxes are subjected to vibrations arising from gear meshing, roller bearings forces and wheel-rail contact. This paper shows how peculiar service conditions made the application of a well known and perfectly working gearbox installed on a metro vehicle rather critical. After a long investigation, the root cause of the problem was found in running conditions at top speed, which happened for long distances in coasting, being a rather long section of the line made of quite distant stations on a mild slope line, a situation that that kind of vehicle never encountered in other lines. Remedies are discussed with reference to mechanical and electric features of the vehicle. The adoption of a new procedure, called "regenerative coasting" allowed to potentially solve the problem of premature failures in service.

Keywords: gearbox, vibrations, bearings, failure, cage, railway, metro, traction control, regenerative coasting, power recirculation.

1 Introduction

Mechanical transmissions are needed in railway vehicles to adapt the engine characteristics to the specific needs either of a locomotive or of a distributed power vehicle (EMU – Electrical Multiple Unit or DMU – Diesel Multiple Unit).

A quite complex transmission is absolutely necessary for Diesel vehicles as this engine is not capable to supply any torque at zero speed. In the case of an electric metro vehicle, wheel diameters and operating speeds are such that the angular speed of wheelsets is rather small, while modern electric motors supply high power as a combination of small torque and high angular speed. As long as torque is somewhat proportional to rotor diameter, the convenience of using small motors rotating fast is evident also because motor self cooling is much easier at high angular speeds, not requiring additional motor fans. As a consequence, metro applications therefore often require a mechanical transmission with a two-stage gearbox. Motors are often connected to bogie frames or even to the carbody and in these cases a joint allowing for misalignments must be included in the driveline. Only in the case of the “tram transmission” simpler solution, the first one that was historically used, there is a direct motor-gearbox connection without a joint. In this latter case the motor is partly hanging on the axle increasing the non-suspended mass.

Gear design and machining always require a certain residual play (or backlash) between meshing gears as they cannot work preloaded. This inevitably introduces a non-linearity in the dynamic behaviour of the gearbox if for any reason the torque changes rapidly its sign passing from traction to braking. As a matter of fact, gearboxes work fine when the torque transmitted is steady and “firm”, meaning that it should be close to design torque and with small variations. The main reasons for this clearly stands in the need to guarantee a proper film lubrication of meshing gears and roller bearings. Continuous reversal of teeth-meshing related forces tend to destroy steady lubrication conditions, exposing the mechanical parts to greater wear and possible premature and unexpected failures.

This paper shows an application case where an EMU trainset was used on a light rail line. Although operating conditions were well inside the design limit of the vehicle and that a fleet of around 40 trains was perfectly running for several years in a conventional metro, the “extension” of the service to a light rail line was harmful for the integrity of gearboxes. After a description of the vehicle and of the service, a number of attempts that were done to solve the problem are discussed until the application of unconventional measures that can completely remove the root cause of the failures.

2 Description of vehicle, lines, service and failures

2.1 Description of the metro vehicle

The vehicle discussed in this work is a conventional metro vehicle with 6 cars, with two bogies each, an axleload of 12 t/axle when fully loaded and a maximum speed of 80 km/h. Line characteristics of the application, discussed later in more detail, are such that a 2/3 traction was sufficient.

The vehicle architecture (Figure 1) is such that a train is composed of two identical Traction Units, each made of a driving trailer and two motor cars. Each train has therefore 8 trailed axles and 16 motor axles. Motor bogie architecture is quite conventional for this class of vehicles, with metal-rubber primary suspensions and air spring secondary suspensions installed on a bolster (Figure 2). Electric motors are installed longitudinally, mounted on a frame that is elastically connected to the bogie frame.

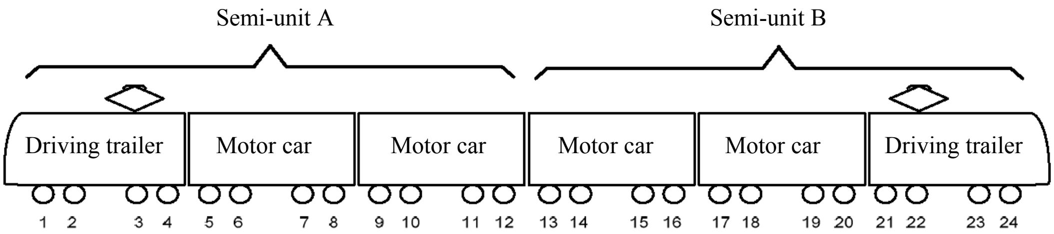

Figure 1: Train symmetric composition (two traction semi-units)

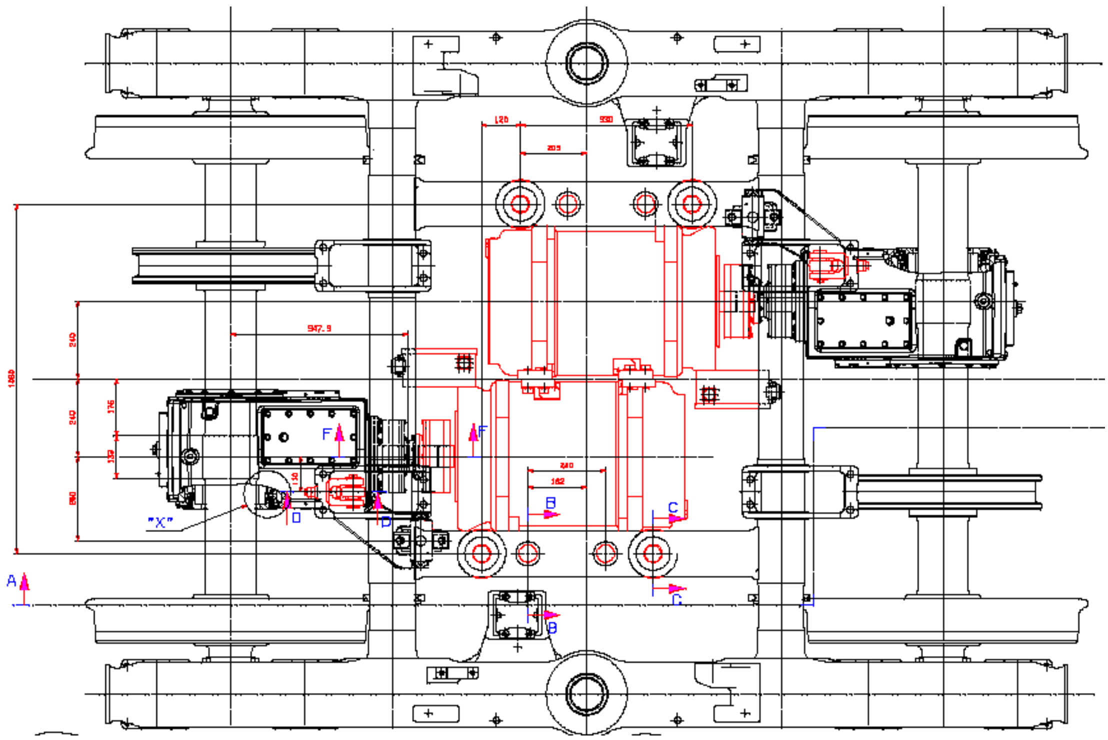

Figure 2: Top view of a motor bogie. Electric motor cases (in red) are mechanically coupled and elastically suspended to the bogie frame. Joints and gearboxes can be easily identified

Gearboxes (Figure 3) include a first stage bevel gear (i_1=21/37) to transmit the motion between orthogonal axes and a second spur helical gear stage (i_2=19/80). Motor-gearbox coupling is guaranteed by a toothed joint which is designed to be torsionally rigid. Torque is reacted by a vertical rod mounted on rubber elements on gearbox case and connected to the bogie frame.

The intermediate shaft is supported by tapered bearings in X-arrangement. With the nominal wheel diameter d=840 mm, rotating speeds at the maximum operating speed of v=80 km/h are f_0=62.5 Hz (3750 rpm) for the input (motor) shaft, f_1=35.5 Hz for in the intermediate shaft and f_2=8.4 Hz for the output (axle) shaft. Corresponding meshing frequencies are f_{m1}=1322 Hz for the bevel gear and f_{m2}=674 Hz for the spur gear.

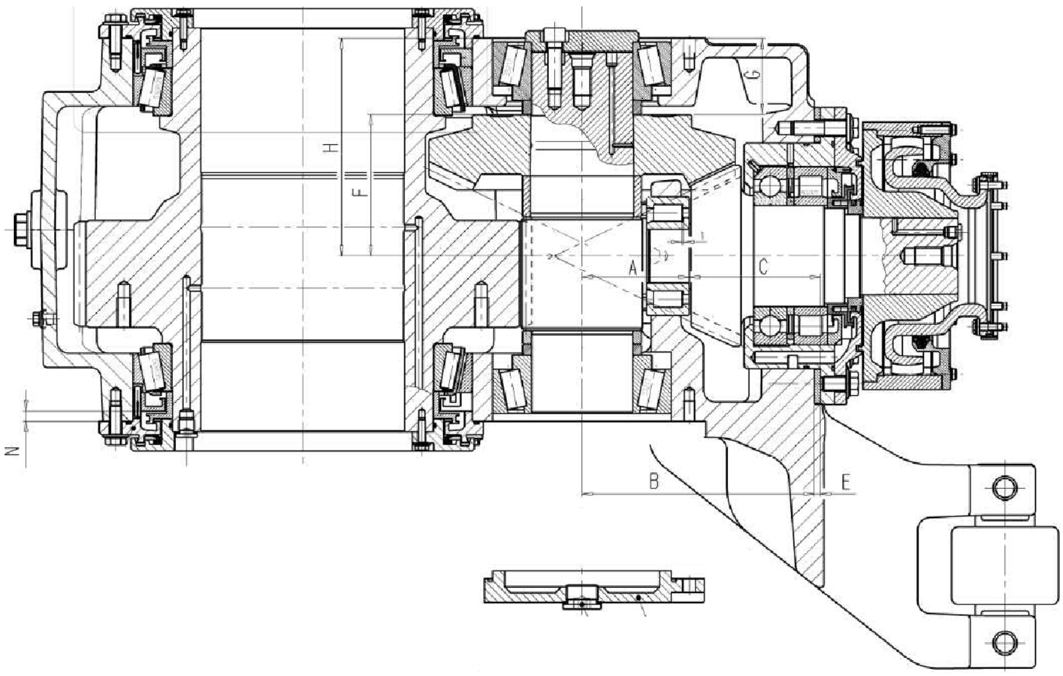

Figure 3: Gearbox section. One of the covers of the intermediate shaft is shown displaced

2.2 Description of the line and service

The vehicles described in this paper are operated on the following lines (Figure 4):

- Line 1: 18.5 km conventional metro line with 27 stations (average distance between station ≈700 m). This is the line on which the vehicles initially operated in a large number (around 40 trainset);
- Line 3: 18.1 km conventional metro line with 22 stations (average distance between station ≈860 m, with peak distances of 1560 m and 1533 m). Vehicles operating on this line come from the previous batch;
- Line 3: 28.4 km light rail line with 14 stations (average distance between station ≈2200 m, with a peak distance of 5692 m and six sections longer than 2 km). These trains (six) come from a further batch.

A distinguishing feature of Line 3 is that it connects two stations at approximately the same level and as a consequence it results to be therefore mainly flat. Nevertheless, almost halfway between terminal stations, there is a hill where the line climbs up and descends with slopes of around 16‰ and 20 ‰ (Figure 5). Both these slopes are largely sufficient to allow coasting; as a common practice, drivers pass the turnouts of the station located on top of the line at around 60 km/h and let the train accelerate downhill to reach the maximum operating speed of 80 km/h.

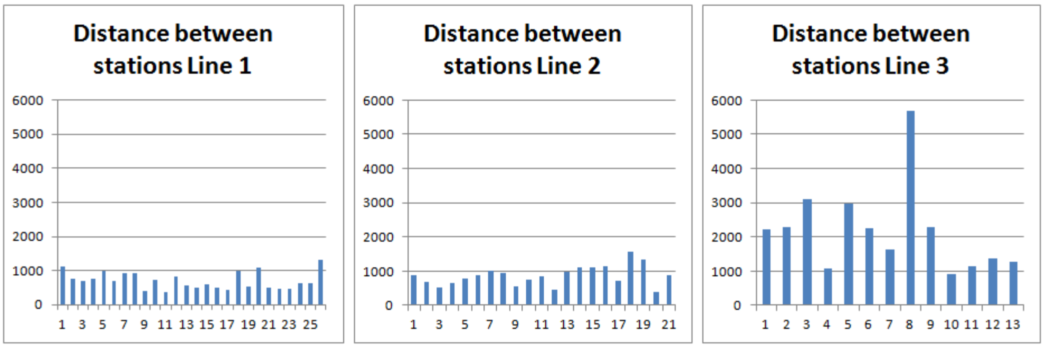

Figure 4: Distance between stations in Lines 1, 2 and 3.

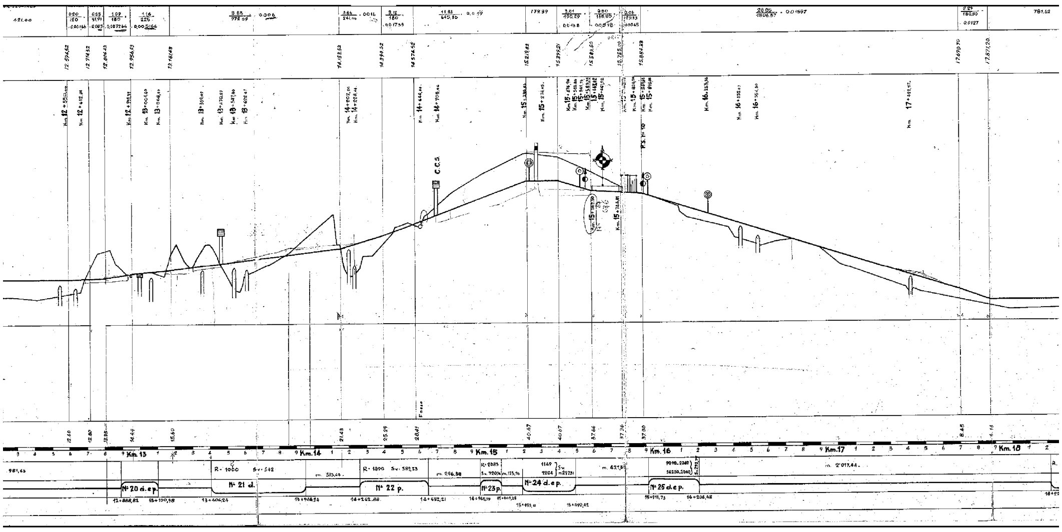

Figure 5: Level of line 3 (close-up to the central hill).

As a result, running conditions of the same rolling stock are rather different between Lines 1-2 and Line 3. This can be seen in Figure 6 where the data downloaded from the “black box” of the vehicle are compared, marking in red points where coasting conditions are found. It emerges that Line 1 has in practice no coasting: the train starts, reaches the maximum speed and stops at the following station. Line 2 has some more coasting between 40 and 60 km/h, while Line 3 has long sections run in coasting at full speed. It is interesting to observe the long acceleration and the long deceleration *during coasting* evident on Line 3 close-up: this is the longest slope seen in Figure 5, run once downhill and once uphill (during the return run). In one case this coasting condition around maximum speed lasts for more than 3 km, a certainly impossible condition to be found in Lines 1 and 2.

Figure 7 gives the different distribution of speed on the three lines. As an example, only 2% is run above 60 km/h for Line 1, while Lines 2 and 3 have figures of 9.5% and 18% respectively. Even more interesting, while there is in practice no statistical relevance for run above 70 km/h for Line 1, this still represents more than 14% for Line 3, and as seen in Figure 6 large part of this mileage is run in coasting.

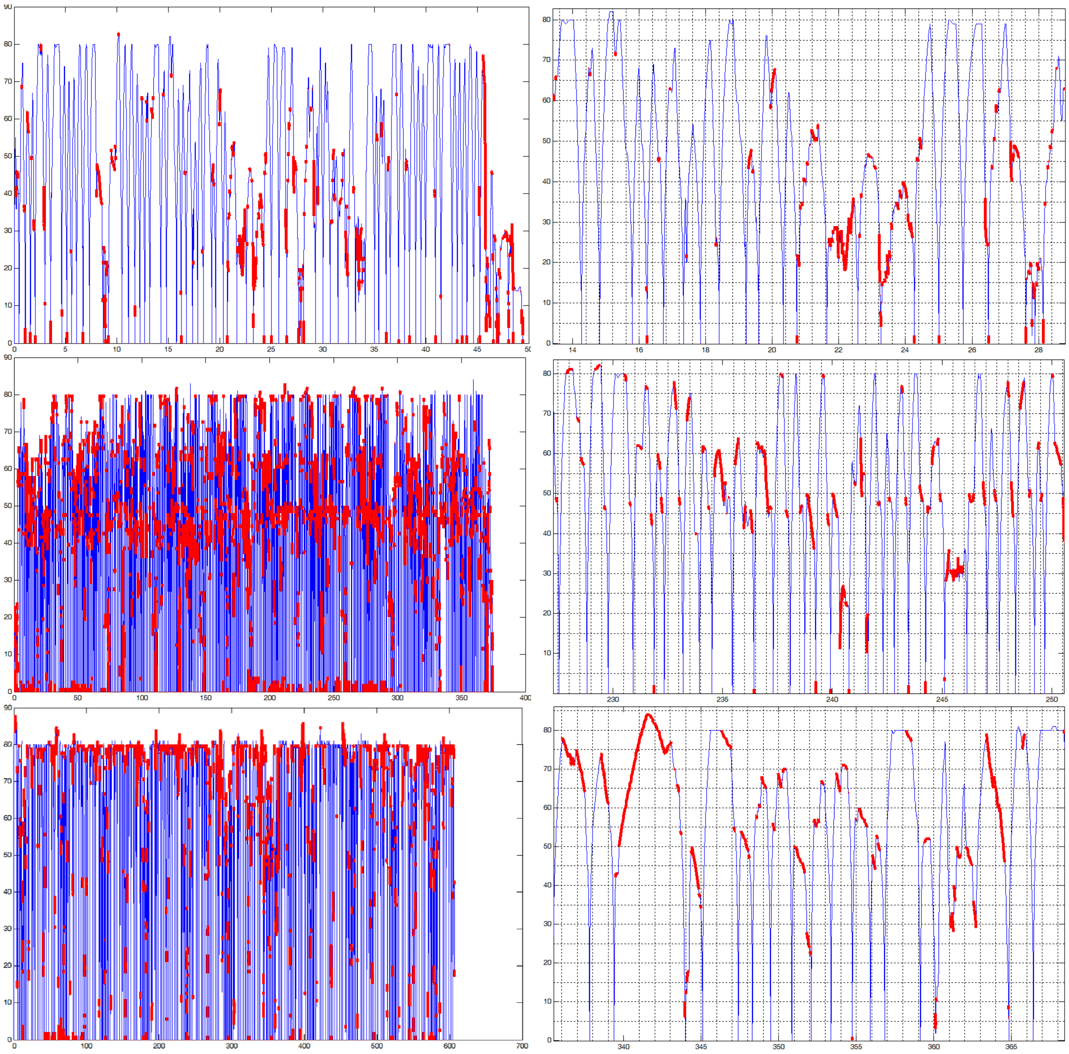

Figure 6: On the left: speed recordings on Line 1 (top), Line 2 (mid) and Line 3 (bottom). Red dots represent coasting running conditions. On the right: close up on a significant portion of the records

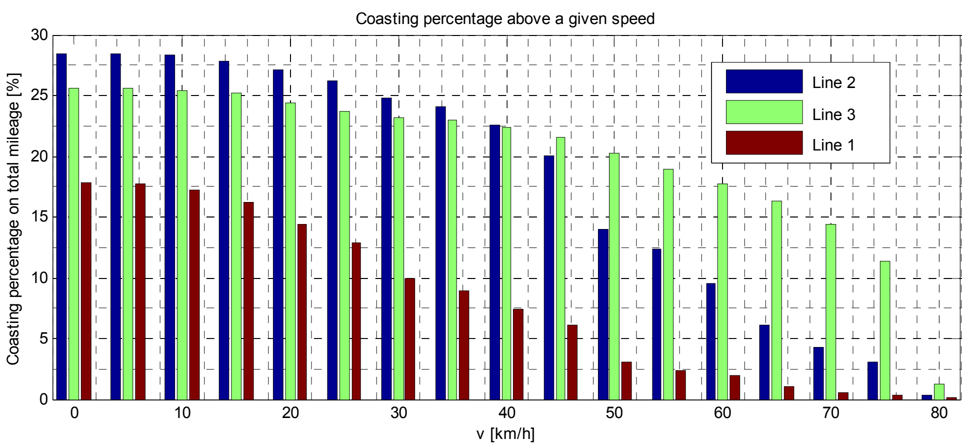

Figure 7: Percentage of mileage run in coasting above a given running speed for Lines 1, 2 and 3

2.3 Description of the failures

As already mentioned, gearbox failures happened for the overwhelming majority of the cases on Line 3. The consist in the break of the cage of the taper roller bearing located on the intermediate shaft, opposite to the bevel gear (see Figure 3). As a precursor of the complete failure, abnormal distortion and wear of the cage can be observed by properly measuring the axial play of the intermediate shaft. Although these checks allowed to completely avoid failures during operations and related consequences, any time an abnormal play is found both bearings of the intermediate shaft are changed with unacceptable material and workforce costs. Although fleet availability was unaffected, the manufacturer was claimed to solve the problem and involved the authors to investigate the root causes of the failures.

2.4 Conditions of the fleet

It is always hard to "freeze" a situation that is continuously changing as long as trains are running daily and the statistics should be constantly updated. To give the reader an idea of how the maintenance operations affected the operational life of the bearings, Figure 8 shows the mileage run by each gearbox running on Line 3 after bearings change as of 15.9.2012 (to further complicate the situation, two trains collided in service and the parts remaining undamaged after the accident were assembled to form a further "hybrid" train).

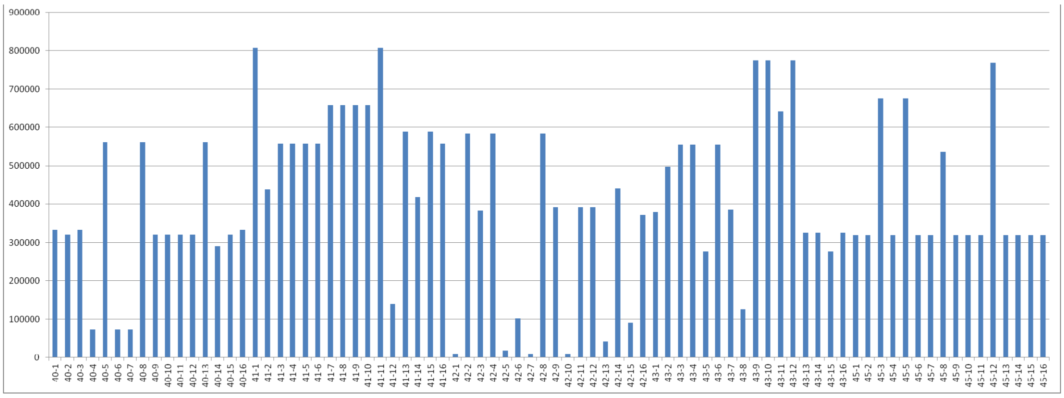

Figure 8: Distance run by each of the 80 gearboxes of the trains running on Line 3 (as of 15.9.2012)

It can be seen that:

- some gearboxes are still in operations from the original supply even if they ran over 700.000 km, some other are "brand new", in the sense that their bearings were changed quite recently;
- the majority of failures happened between 200.000 and 400.000 km, while the original interval forecasted for general overhaul of the gearbox (when bearings had to be checked) was originally set to 1.2 million km.

Both these evidences indicate that the problem in subtle and tricky: not all of the bearings of the first supply failed (and when they are still in service they clearly completed the highest run), while just repaired gearboxes are not interesting as they are “new”. Figure 9 shows the data aggregated by original bearings, OEM changed bearings, and alternate supplier changed bearings.

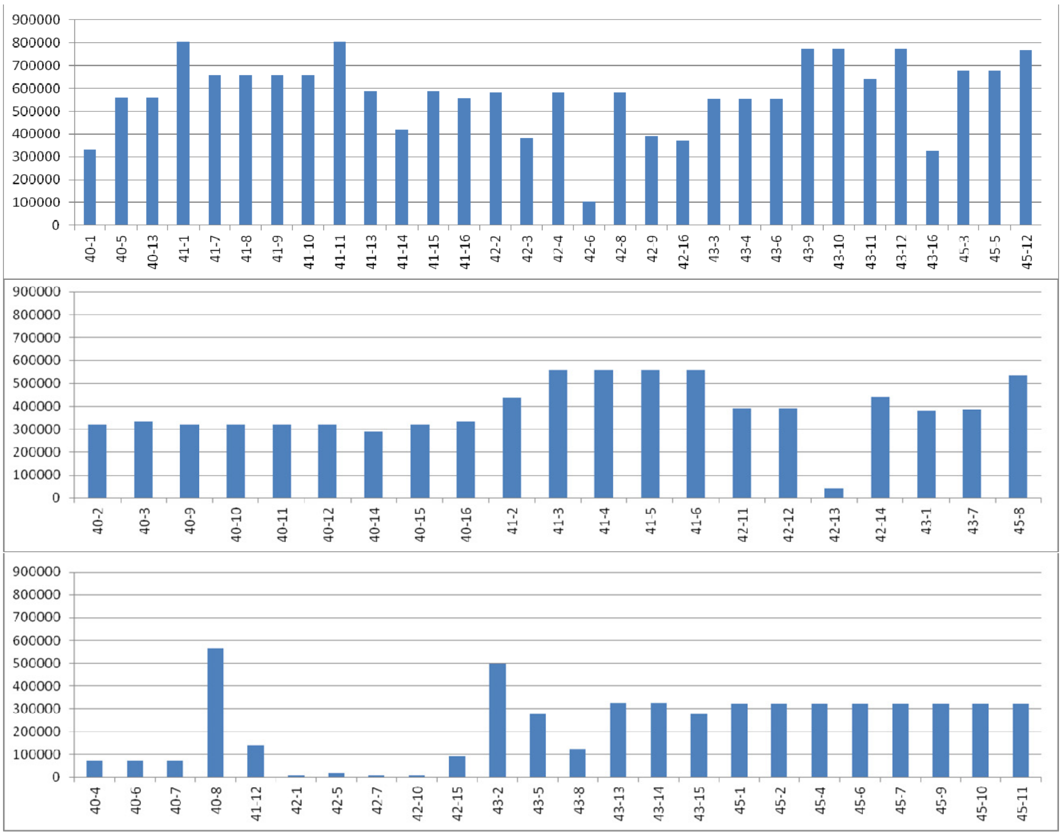

Figure 9: Distance run by original (top, 31 gearboxes), retrofitted with OEM bearings (mid, 21 gearboxes) and retrofitted with alternative supplier bearings (bottom, 28 gearboxes) gearboxes as of 15.9.2012 for trains running on Line 3

3 Experimental activities

3.1 Initially available data

As known, the best sensor to monitor the conditions of a running equipment is the accelerometer. Several measurements were available when this work was started, all of the them reporting “erratic spikes of high level” during both test runs and normal operation conditions. An example of what was observed is shown in Figure 10, where gearbox vibrations are compared to forces measured by using strain gauges bonded to the reaction rod. It looks clear that the reaction rod forces changes regularly its sign, showing a vertical oscillatory movement of the whole gearbox. Packets of vibrations is coasting contain both gear meshing frequencies.

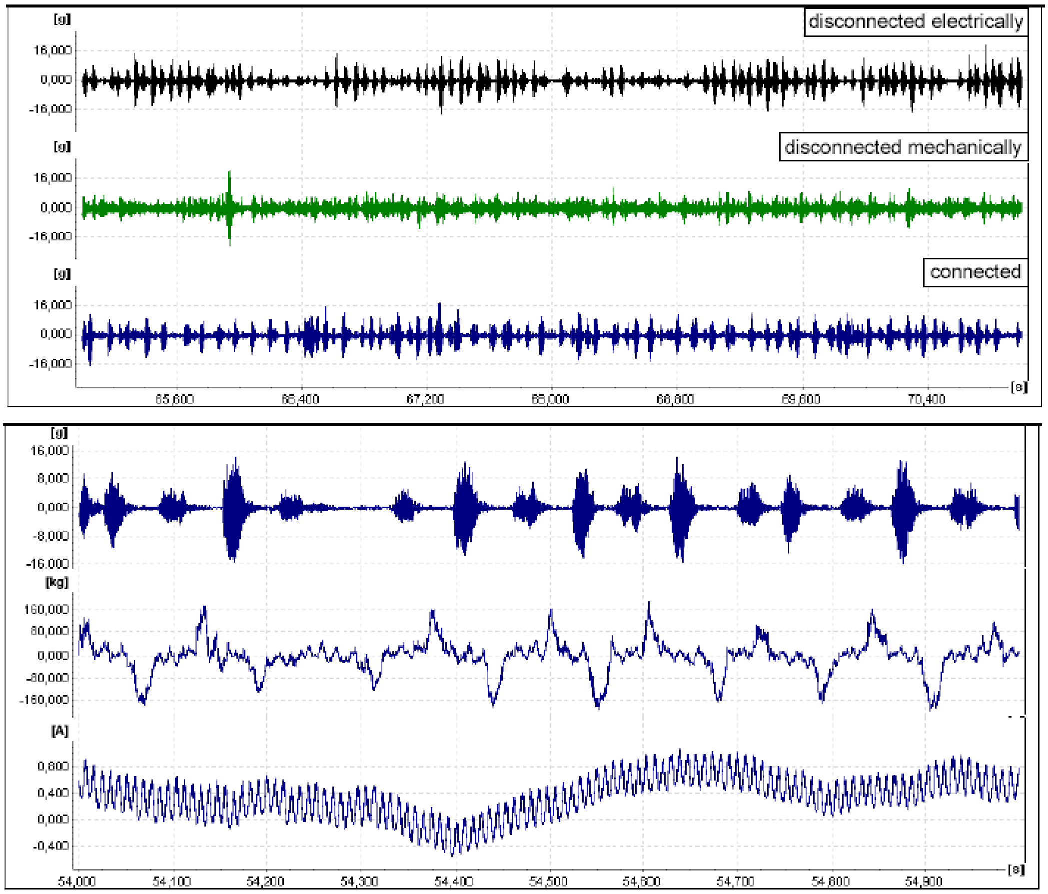

Figure 10: Vibrations in coasting at around 80 km/h. Top: accelerations recorded when motor and joint are electrically disconnected (inverter off), mechanically disconnected (joint opened) and connected (inverter on). Bottom: vibrations of the gearbox, stresses in the reaction rod and motor current

3.2 Test campaigns 1 and 2 (July and December 2010)

An approximately 7 km long section of the track of Line 3 was found defect free by measuring axlebox accelerations on a driving trailer at v=40 km/h (a_{RMS}=0.5÷1 g with peaks of ≈±5 g) and this section was selected for all further tests (Figure 11).

Tests were initially performed on a gearbox that had run approximately 90.000 km with new bearings. The presence of spikes was readily found; these were more present with inverter switched off than with the inverter switched on; an example of spikes found is shown in Figure 12, where very high top levels (up to 70÷80 g) were found. As long as vertical movements were apparently involved, the joint was disconnected and an excitation with an instrumented hammer was given while the response was measured with an accelerometer mounted near the reaction rod attachment (Figure 13), measuring the point frequency response function (inertance) of the whole gearbox.

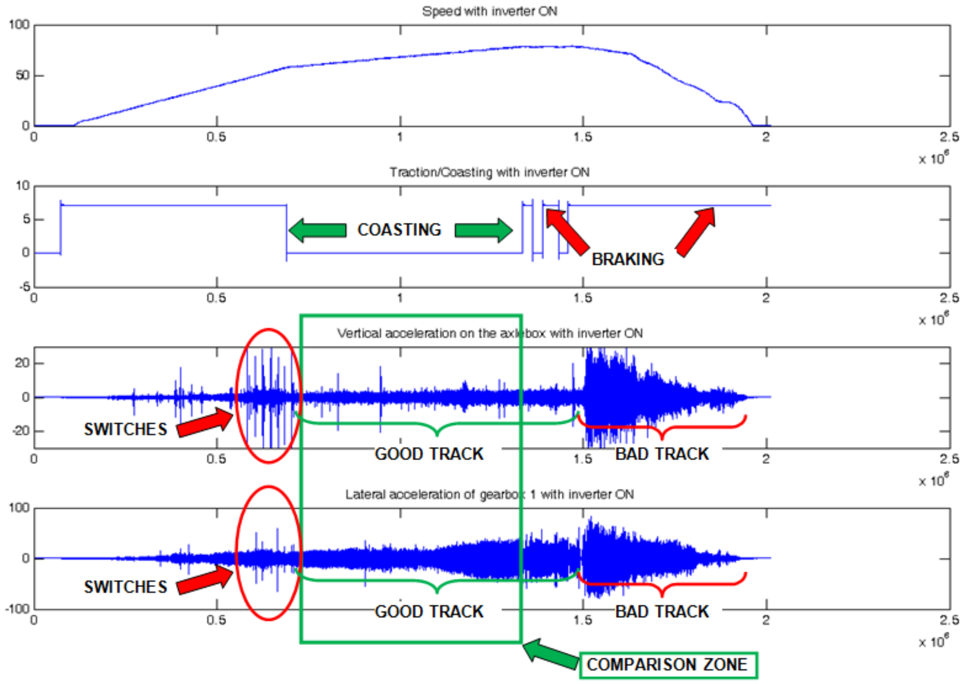

Figure 11: Axlebox vertical acceleration and gearbox lateral acceleration records to identify the best track section

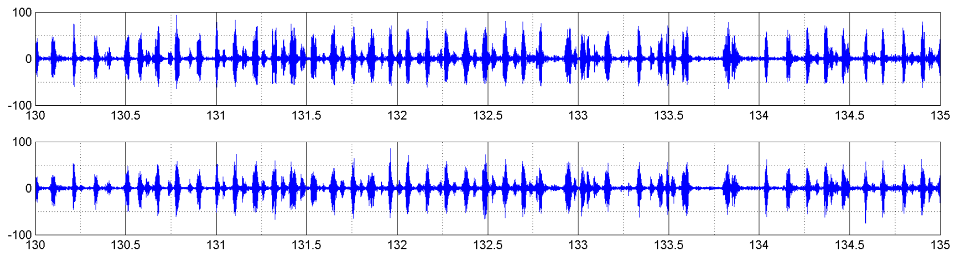

Figure 12: Lateral and vertical accelerations recorded on a gearbox in coasting at 80 km/h (gearbox age: 90.000 km)

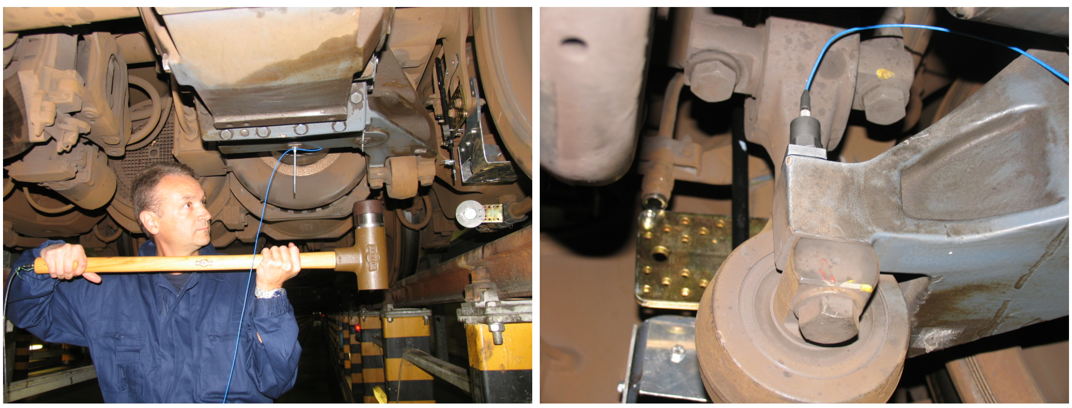

Figure 13: Vertical excitation with instrumented hammer (left) and measuring accelerometer mounted close to the reaction rod attachment (right)

As long as acceleration spikes number and amplitude were found to both increase with speed (Figure 14), a deeper analysis of the data led to the conclusion that there was a relationship between the vertical resonances of the gearbox and the acceleration levels recorded during test runs. As shown in Figure 15 and in Figure 16, the correlation between maximum acceleration values and the highest peak in the gearbox vertical response was clear.

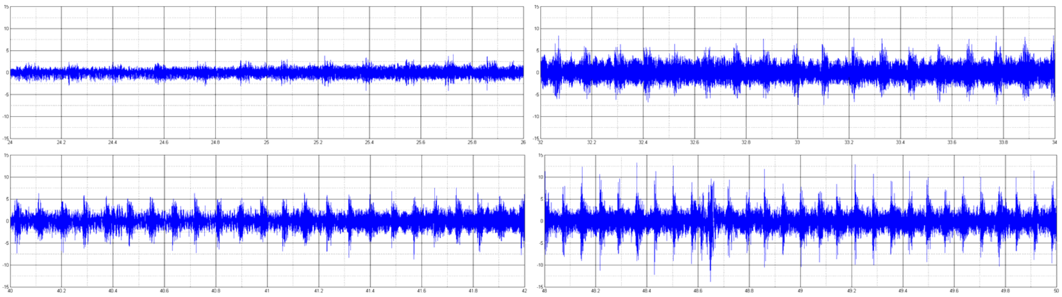

Figure 14: Accelerations recorded at the reaction rod attachment at v=30 km/h (f=6 Hz), v=45 km/h (f=9 Hz), v=58 km/h (f=11.5 Hz) and v=72 km/h (f=14 Hz)

As the importance of gearbox natural frequencies was evident, all the gearboxes of a different train were tested with the impact hammer, leading to the results shown in Figure 17. All the gearbox appeared very similar, leading to the conclusion that the failures were possibly due to the coincidence of the forcing function and the natural frequency of the gearbox (resonance condition). Eight gearboxes of this train were therefore equipped with accelerometers and measured but the data were unusable as *all channels saturated the ±50 g range*, showing damages in all the gearboxes.

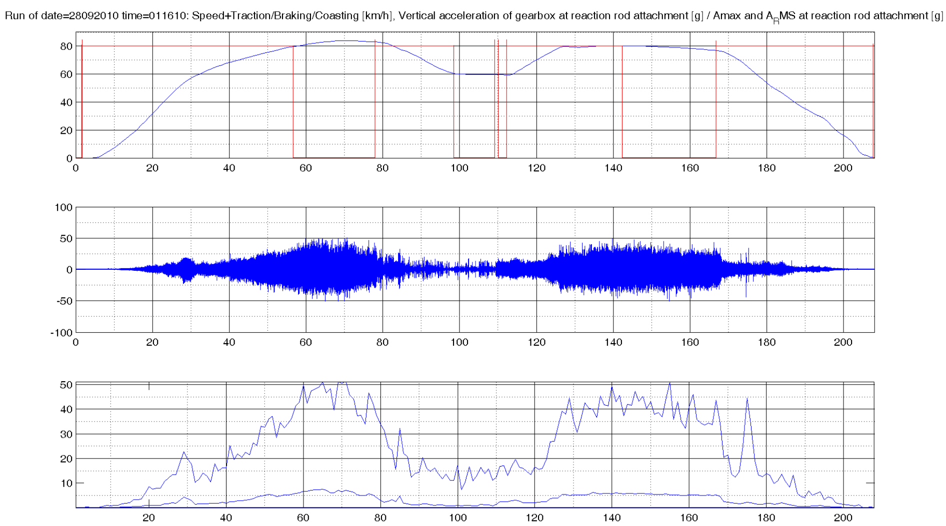

Figure 15: Signals recorded during a full test run. Speed & coasting signal (top), acceleration on the reaction rod (mid), RMS and peak of acceleration (bottom) (1 s interval)

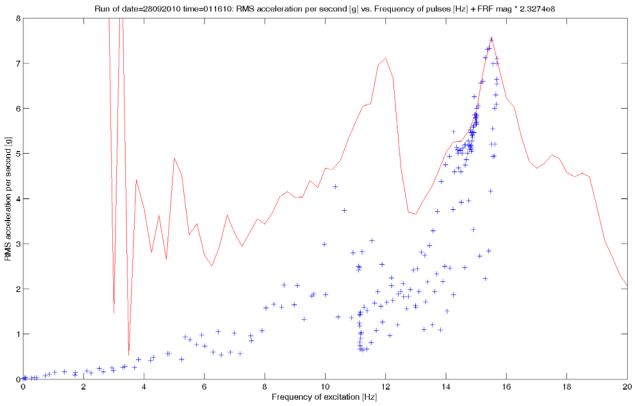

Figure 16: Signals recorded during a full test run. Frequency response function measured with impact hammer (red, joint disconnected) compared to RMS energy as a function of frequency (=speed)

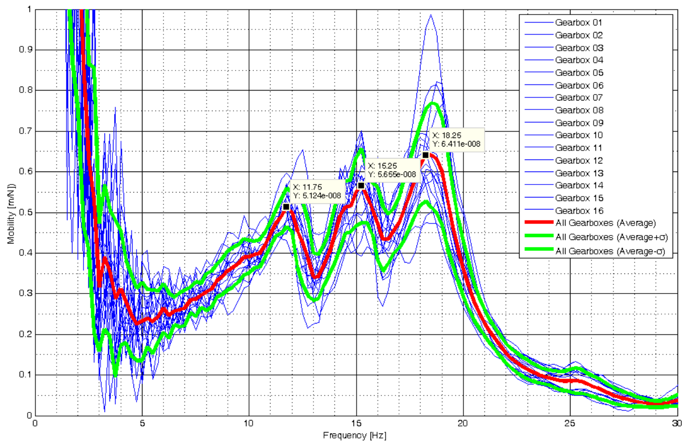

Figure 17: Frequency response function of all the gearboxes of a train. Joint is connected

3.3 Test campaign 3 (January 2011)

Tests were repeated on a different train and, quite surprisingly, the accelerations did not show any clear relationship between amplitude and frequency with speed and the spikes were again quite erratic (Figure 18). It was therefore concluded that the results found before were only due to a gearbox *that was already damaged* at the time of the measurements. The hypothesis of a root cause due to resonance was therefore discarded: the dynamic system was *tuning itself on the vertical natural frequencies that "drove" the system to oscillate at that frequency and to produce spikes at that frequency*. When the damage was removed, by choosing a different train, that coincidence disappeared. Reversing from traction to braking the torque in the gearboxes, different teeth flanks meshing conditions (see Figure 19) led to clear changes in the average acceleration levels (Figure 20). Different meshing conditions also affected vibrations during coasting (Figure 21).

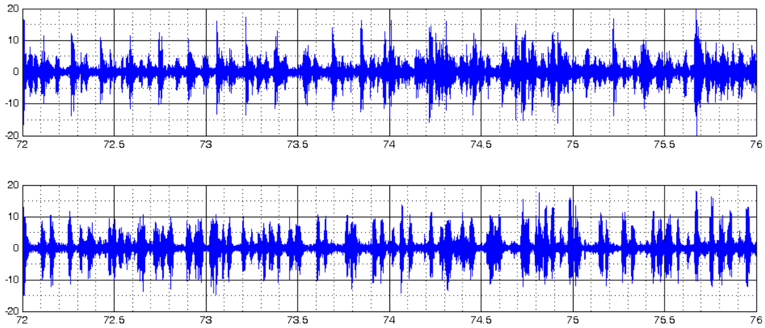

Figure 18: Erratic acceleration spikes measured near the reaction rod attachment during a run at 60 km/h in January 2011. No clear relationship with speed was found

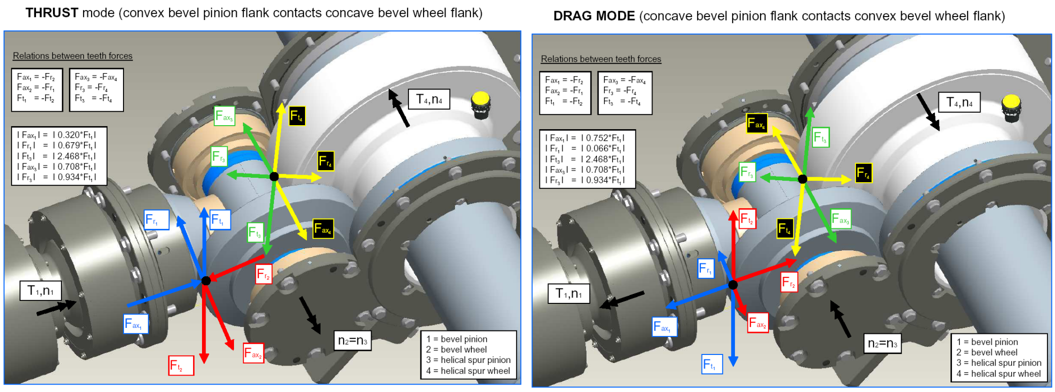

Figure 19: Definition of thrust and drag modes of the gearboxes

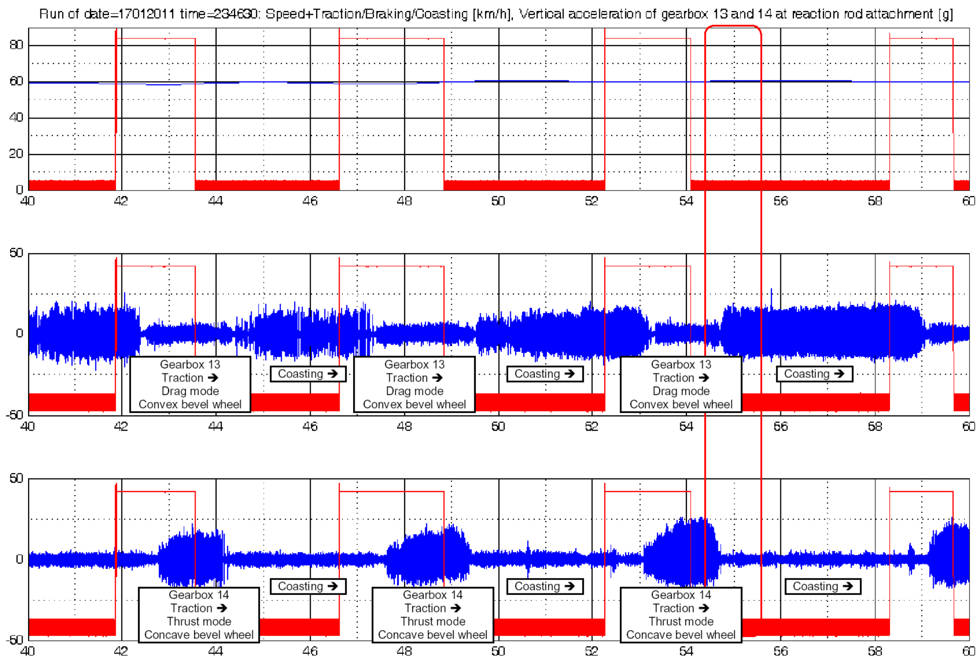

Figure 20: Acceleration levels during thrust and drag mode for two gearboxes (A and B) belonging to the same bogie

GEARBOX A

Direction	Eastbound			Westbound		
Running conditions	Coasting	Traction	Braking	Coasting	Traction	Braking
Gearbox Condition and rotation direction	--- ↺	DRAG ↺	THRUST ↺	--- ↻	THRUST ↻	DRAG ↻
Active flank of bevel wheel	---	Convex	Concave	---	Concave	Convex
F_{IS}	---	0.774 F_{t1}	-0.029 F_{t1}	---	-0.029 F_{t1}	0.774 F_{t1}
Axial load on intermediate shaft	---	Loaded	Unloaded	---	Unloaded	Loaded
Load on the reaction rod	↓	↓+⬆	↓+⬇	↓	↓+⬇	↓+⬆
Vibration level	HIGH	⇩	⇔	LOW	⇧	⇩

GEARBOX B

Direction	Eastbound			Westbound		
Running conditions	Coasting	Traction	Braking	Coasting	Traction	Braking
Gearbox Condition and rotation direction	--- ↻	THRUST ↻	DRAG ↻	--- ↺	DRAG ↺	THRUST ↺
Active flank of bevel wheel	---	Concave	Convex	---	Convex	Concave ↻
F_{IS}	---	-0.029 F_{t1}	0.774 F_{t1}	---	0.774 F_{t1}	-0.029 F_{t1}
Axial load on intermediate shaft	---	Unloaded	Loaded	---	Loaded	Unloaded
Load on the reaction rod	↓	↓+⬇	↓+⬆	↓	↓+⬆	↓+⬇
Vibration level	LOW	⇧	⇔	HIGH	⇩	⇔

Figure 21: Vibration behaviour of gearboxes in thrust and drag modes measured during several test runs in both directions

4 Several fruitless attempts to avoid spikes

4.1 Increase of the reaction rod stiffness

Although gearboxes with bearings in good conditions do not exhibit resonances as they are not defective, a fundamental result to achieve was the avoidance of the coincidence of forces generated inside the taper bearings with defects and the vertical resonance frequencies of the gearbox.

The frequencies due to possible defects on the rollers and on the races (*BPFO*= ball pass frequency on outer race, *BPFI*= ball pass frequency on inner race, *BSF*= ball spin frequency, *FTF*= fundamental train frequency) were all analysed for the taper bearings of the intermediate shaft and a proposal to increase the stiffness of the rubber elements of the reaction rod was made to shift outside the range of normal speed the excitation frequency of the *FTF*, which is related to defects in the cage (Figure 22).

The attempt to install a modified reaction rod including all-steel spherical joints (Figure 23) failed due to too high play inside the joints that are very stiff but that cannot be effectively adjusted (or preloaded) in this application. Nevertheless, the use of a different rubber (without play) element should be considered carefully in case of retrofit of the gearbox fleet.

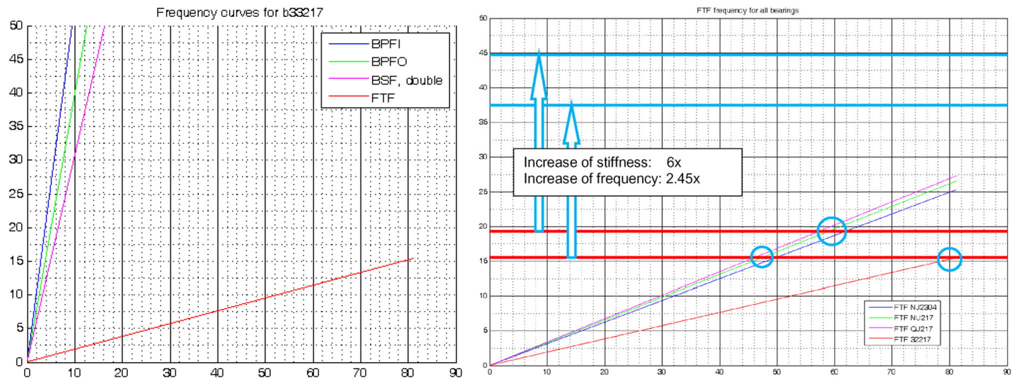

Figure 22: Passing frequencies [Hz] in taper roller bearings of the intermediate shaft vs. speed [km/h] (left). Effect of increase of the vertical stiffness on vertical natural frequency of the gearbox compared to FTF frequencies of all bearings inside the gearbox (right)

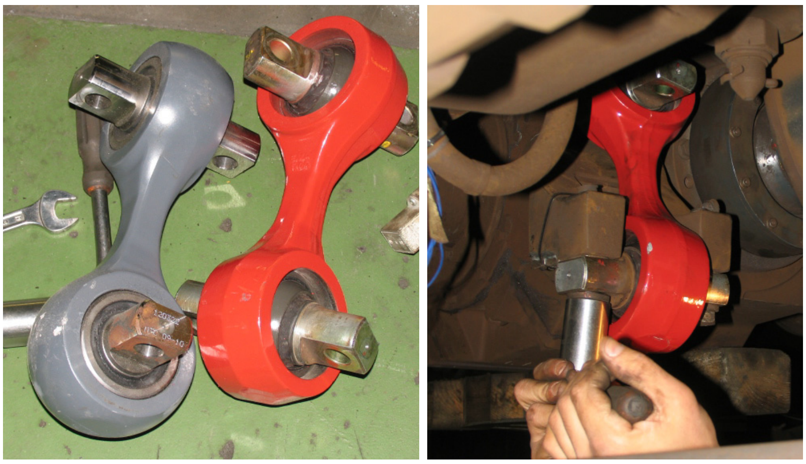

Figure 23: Standard rubber joints (grey) and stiffened all-steel joints (red) reaction rod. No fixed position of the joint is defined as both joints are free to rotate

4.2 Variable hydraulic preload of the intermediate shaft

In order to try to reduce variations in the load ("shaking") of the intermediate shaft, an axial preload system was designed and built. By modifying an intermediate shaft cover, eight hydraulic pistons were introduced to give forces on the outer race of the taper bearing (suitably ground to allow its axial movement) of up to almost 10 kN, driven by a hand pump (Figure 24). Pressure was monitored with a pressure gauge and a transducer. Although the equipment proved to be easy to install and perfectly working, no differences were obtained during tests, in the sense that peaks occurrence remained unchanged in terms of randomness and amplitude. This evidence was nevertheless useful as it proves that acting on bearing preload or play leaves the source unaffected. Play can certainly exacerbate the problem but it's not its root cause.

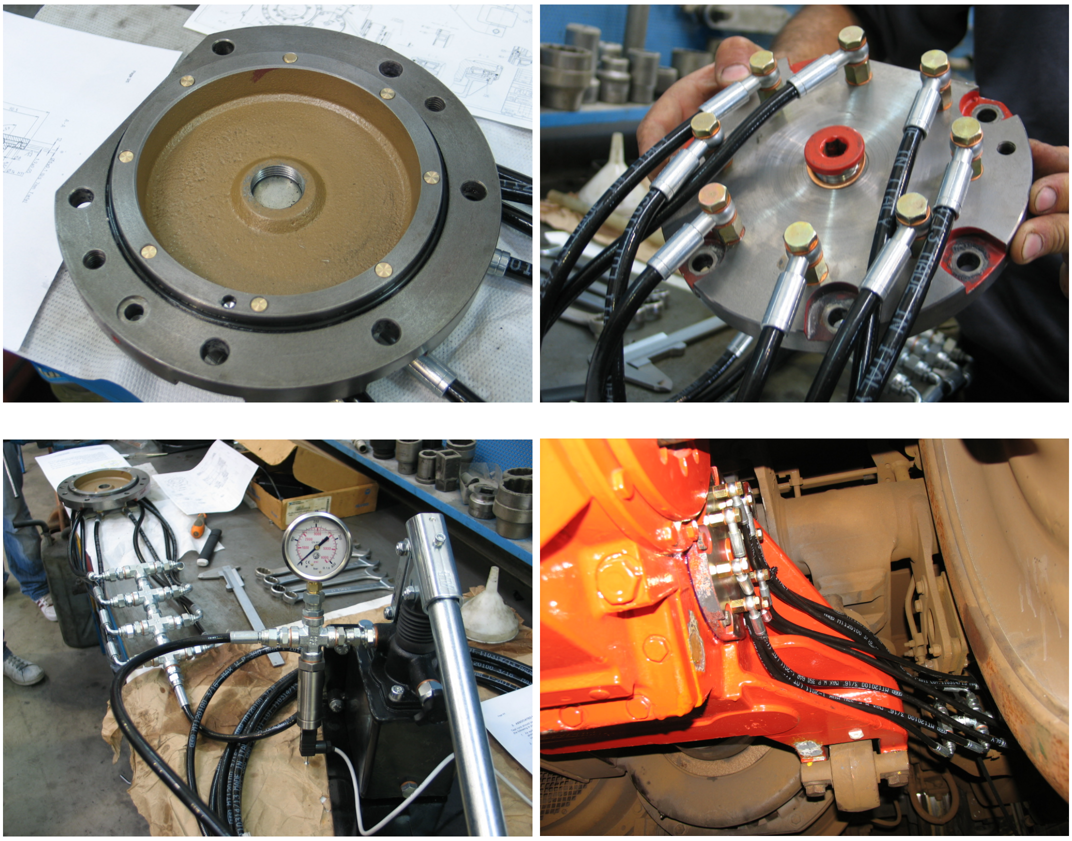

Figure 24: Intermediate shaft cover with 8 hydraulic pistons to push axially the outer race of the taper bearing. Details of the hydraulic pump with pressure gauge and pressure transducer and installation on a gearbox

4.3 Axial and torsional preload of the joint

The joint connecting the motor and the gearbox is shown in Figure 25. It is a torsionally rigid joint with spherical gears acting on internally splined shafts. This joint is very often used in this kind of applications, as it effectively decouples the motor (which is connected to the bogie frame) and the gearbox (which embraces the axles and is suspended by the reaction rod). Motor and gearbox vibrations have in fact similar levels but different frequency content and the coherence between the two signals is always very low. Motor vibrations are random in nature while gearbox vibrations are dominated by meshing frequencies of the two gears (Figure 26).

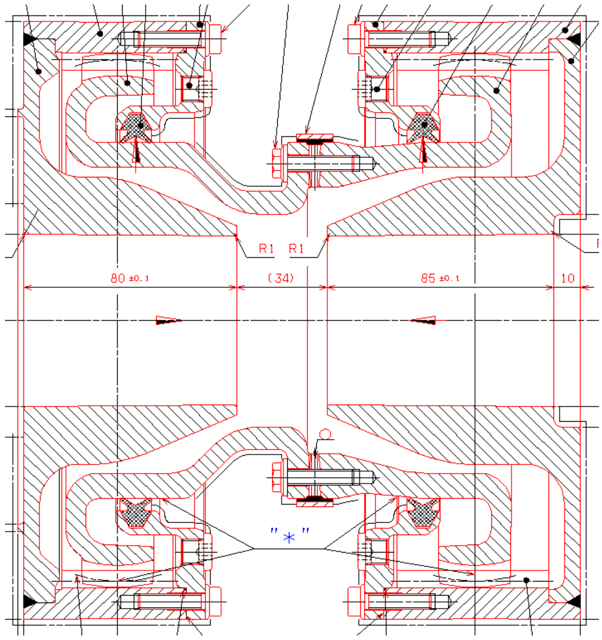

Figure 25: Motor-gearbox toothed joint.

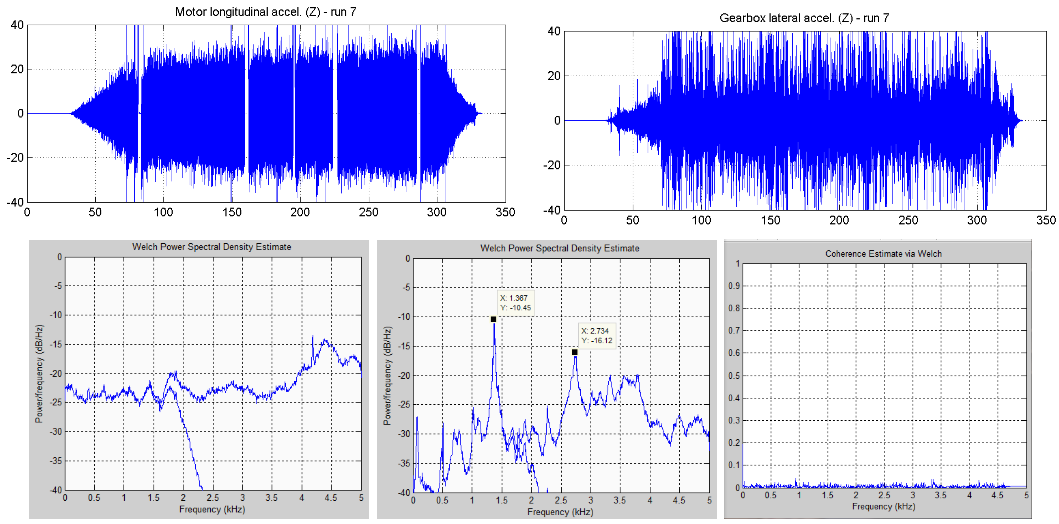

Figure 26: Top: motor (left) and gearbox (right) accelerations (inverter off, 80 km/h). Bottom: Motor (left) and gearbox (centre) acceleration PSD estimates and coherence (right)

To exclude in principle any influence of the possible plays inside the joint, a set of springs giving a torsional preload between the two flanges of the joint was designed, fixing at the same time the axial position of the central toothed element which is free to move along its axis, while a set of further helical springs preloaded the joint with an axial thrust virtually eliminating any play during coasting on bearings of both input shaft of the gearbox and on the motor shaft (Figure 27). Also in this case no appreciable changes in the behaviour of the system were observed, meaning that the attempt to stiffen the connection between the motor and the gearbox is useless to solve the problem.

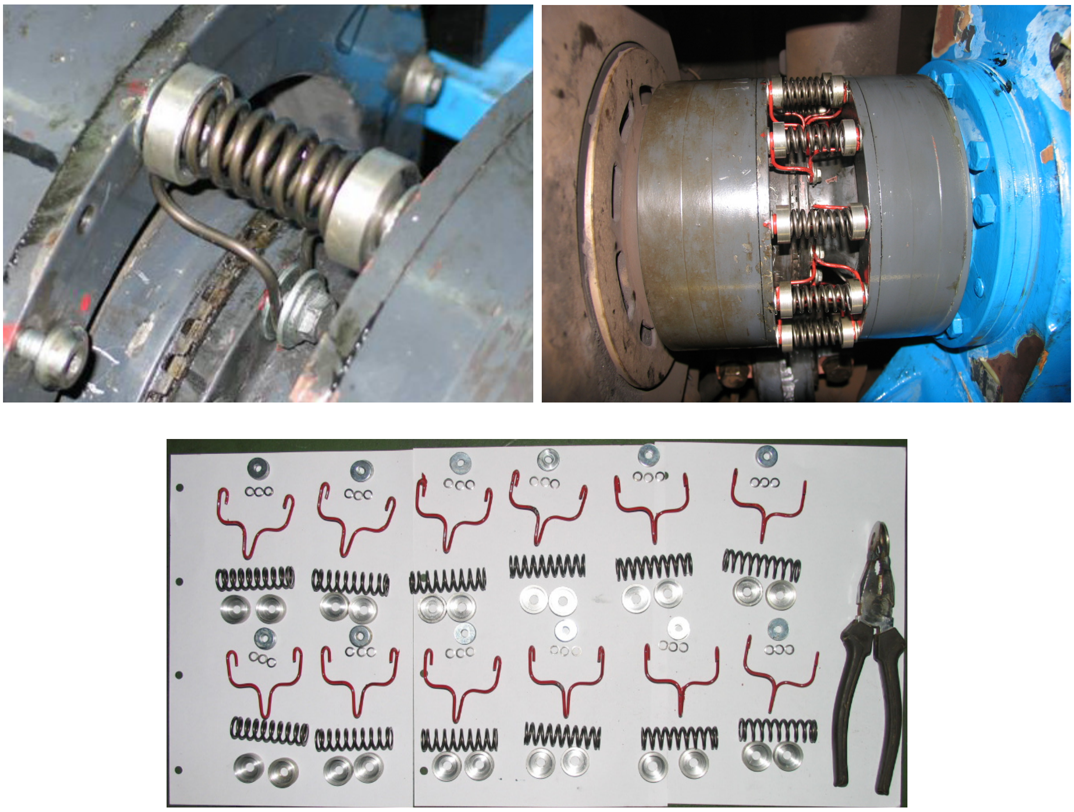

Figure 27: Torsional and axial pre-load “Y” and helical springs during installation

4.4 Change of the joint with similar type

Although there was apparently no reason to make this attempt, a joint manufactured by a competitor was tested on the vehicle. No changes were observed during subsequent tests, and they are not further described in this paper.

5 Analysis of the driveline

At the light of all the tests performed some *ad interim* conclusions were reached, thanks also to the re-analysis of the performance of other vehicles with the same architecture where the “spike phenomenon” appeared constantly.

In the current drawing the joint connecting the pinion of the bevel gear and the rotor of the motor type is a double-spherical joint which moreover allows a relative axial displacement. It is similar to the Cardan shaft with Hooke (universal) joints but it is homokinetic like the Constant Velocity joint. As the joint can transmit neither bending in any plane passing through the motor-gearbox axis nor any force (either axial or radial), the only "generalized force" component that can pass through the joint is a torque which can be considered as the combination of a constant (average) value M_0 and a variable instantaneous value $M(t)$. While the constant torque is responsible of accelerations of the whole vehicle, torque fluctuations will have the only effect of instantaneously changing the angular (rotational) speed of the rotor and, as a confirmation, no evidence of gear meshing is visible in the signals from the accelerometers mounted on the motor. These small angular velocity variations are very difficult to measure.

A completely different situation happens to the pinion of the bevel gear. As in this case the teeth are inclined, when a torque is applied to the pinion shaft a force with all three mutually orthogonal components arises. If the torque is constant these three forces are constant, while if the torque changes its sign, and this normally happens when the vehicle is in coasting (i.e. it transmits no net torque, M_0=0), the three forces reverse and this justifies the large vibrations in all directions observed in the gearbox case in presence of a torque oscillation.

The motor shaft, the joint and the pinion of the gearbox can be seen as a mass (moment of inertia) which can fluctuate around its average central position when running in coasting. As meshing conditions are different in the two directions (drag and thrust modes), this rotor "bounces" between the two meshing conditions when in coasting. It is important to highlight how track irregularities can trigger the bouncing conditions. Longitudinal level irregularities (e.g. joints and switches and crossings) produce a vertical movement of the wheelset and a consequent rotation of the pinion shaft. This can either instantaneously accelerate / decelerate the motor or recover / free the play between the teeth of the bevel gear. Defective track results in more "spiky" operation of the gearbox in coasting.

This analysis of the driveline is heavily conditioned by the presence of play in the gears. Both changing the stiffness in the intermediate shaft ("hydraulic cover") and in the input shaft ("springy joint") gave no results. As long as adding mass to the system is not feasible, the only remaining possibility to influence the behaviour of the system in bouncing / resonating conditions was to add some damping and/or to preload the input shaft. This was expected to have a good efficiency on one side by reducing the amplitude in resonance conditions and on the other side by avoiding as much as possible the appearance of the "bouncing".

6 Damping and torsional preloading the input shaft

Several options were considered to add some damping and preload (braking) torque to the input shaft (eddy current, viscous, friction, aerodynamic). It should first of all be considered that at the top speed (80 km/h) the motor shaft runs at 3850 rpm and that electric current is zero when running in coasting.

After a preliminary study indicated as non-feasible the use of eddy current brakes, the application of a complete disc brake system of a high-performance motorbike was developed. The components were machined and adjusted to be installed on a half-joint flange (Figure 28 and Figure 29). This proved to be the lower cost and best efficiency short-term solution to add (friction) damping to the input shaft. Braking forces are such that a radial component is introduced, together with a braking torque and the desired level of friction damping.

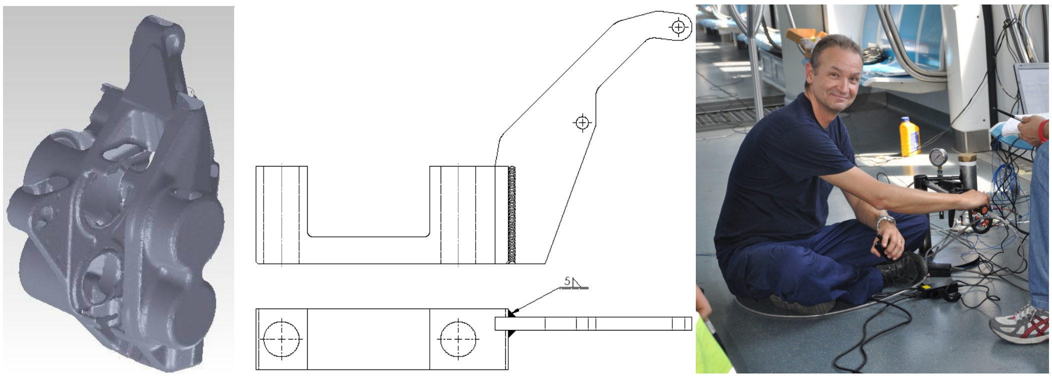

Figure 28: 3-D scanning of the chosen brake calliper with opposed pistons (left) and supporting structure (mid). On-board equipment with motorcycle brake pump and pressure gauge & transducer (right)

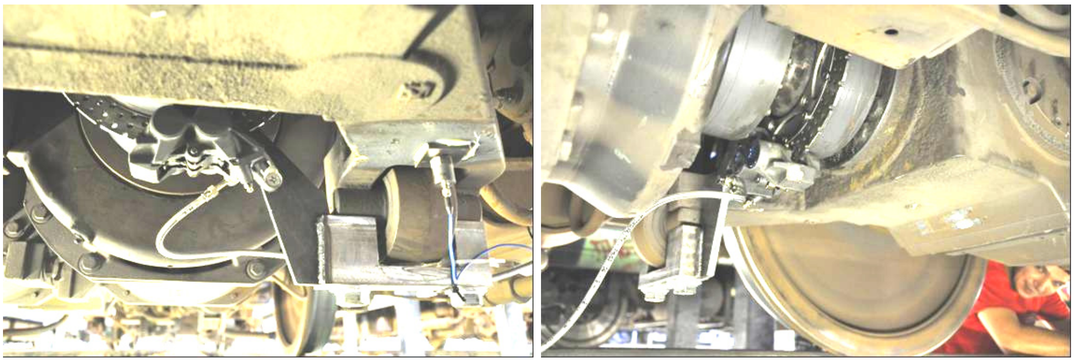

Figure 29: Application of the braking system on the output motor shaft (half-joint flange)

Tests were performed in August 2012 in a specific track in a depot, up to a maximum speed of 60 km/h. The track was preliminary qualified in terms of defectiveness by using the criterion described above. An example of the results is shown in Figure 30 and in Figure 31. It is evident that the braking system introduces large modifications in the vibrations measured on the gearbox, changing the shape of the signals and their frequency content. The companion paper [1] discusses the application of an original signal processing procedure to the data from this measurement campaign and also to the previous ones to check its soundness and its general applicability.

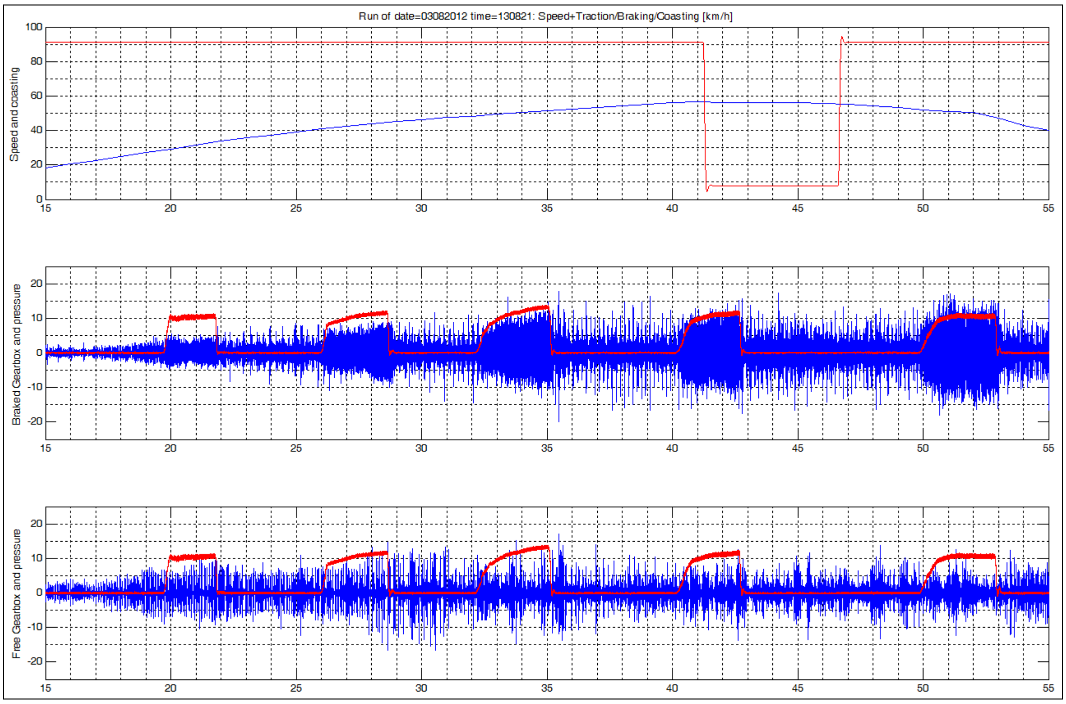

Figure 30: Top: speed and coasting signals. Mid: acceleration of the “braked” gearbox (mid) with pressure in the braking system (in red). Bottom: accelerations of the reference gearbox (bottom, pressure signal in red for reference only)

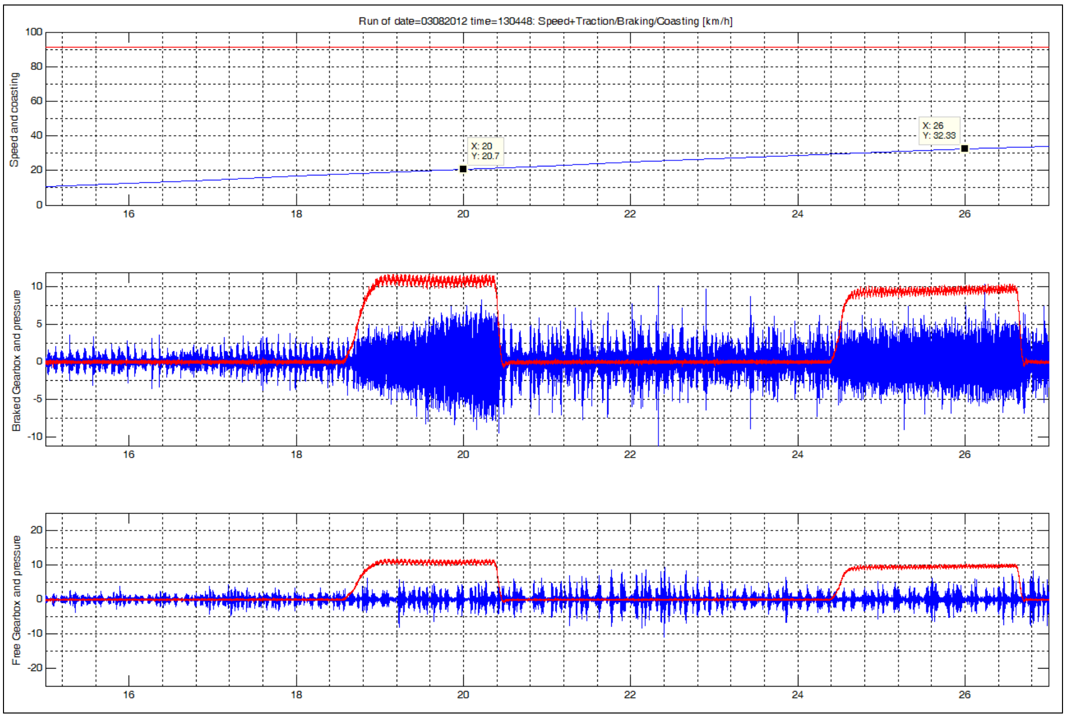

Figure 31: Close-up of a low-speed test run highlighting the influence of braking on acceleration signal measured on braked gearbox (mid trace)

As a result, braking and torsional preload increase energy level of vibrations (RMS value) but decreases the “spikiness” that can be evaluated by using the kurtosis function. These tests were considered therefore very promising showing that such a system positively affects the bouncing behaviour of the gearbox. Although the test system is definitely not applicable as a retrofit to the fleet, its validity as a demonstrator remains unchanged.

7 “Regenerative coasting” as the solution of the problem

Once it was realised that a torque and/or damping can totally avoid the presence of spikes, the authors proposed to the train manufacturer a possible solution based on power recirculation that is explained in Figure 32.

Let’s suppose that the train is in coasting at a speed higher than a selected threshold, that for the goal of this demonstration can be set at any nonzero value but that for safety reason was later fixed at 40 km/h. When the driver moves the manipulator from traction / braking to the “coasting” position, the following phases happen:

- the rear semi-unit (A, in this case) starts braking electrodynamically with a predefined fraction of the maximum braking effort, generating a certain current with a voltage which is sufficient to be fed back to the overhead line;
- the current flows from the rear pantograph to the front one, feeding the front part of the train;
- the front semi-unit (B, in this case) collects the current from the pantograph giving an identical level of traction;
- by simply deriving from the overhead line the (minimal) energy lost in the conversions, this process, named “regenerative coasting”, can give a predetermined preload to all the gearboxes in the train;
- the resulting force of the coupler is a fraction of its design value and has therefore no influence of its fatigue life.

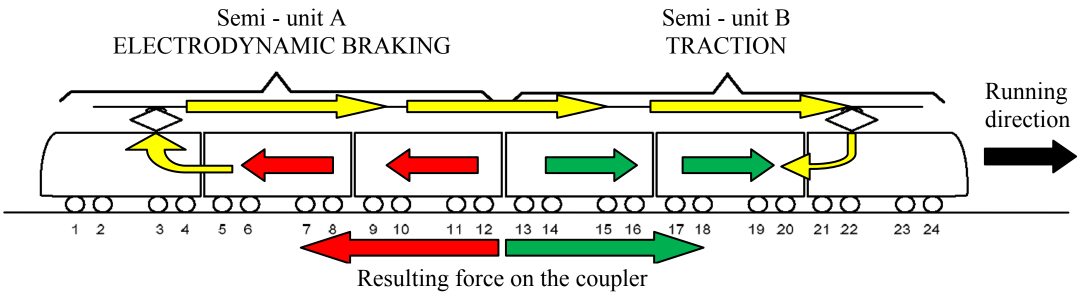

Figure 32: Explanation of the “regenerative coasting” process with braking forces (red), traction forces (green) and current flowing on the overhead line (yellow). Resulting force on the central coupler is also indicated

Regenerative coasting has the great advantage that can be implemented by making quite simple modifications to the traction software that do not affect safety (traction or braking portions of the software remain unchanged). Retrofit to a fleet simply requires the upload of a revised version of the software via an Ethernet cable.

Regenerative coasting was first applied during a recent test campaign held on a vehicle that has an architecture identical to the one analysed in this paper. The vibrations of only four gearboxes (G1 and G2 opposite to G3 and G4) were monitored with different percentages of regenerative coasting (0, 10%, 20%, 30% and 40%) while running in both directions. The results are summarized in Table 1, where the quality of the vibrations was defined according to the following values of the kurtosis function:

- $k < 2.5$ very good behaviour (++);
- $2.5 \le k < 3$ good behaviour (+);
- $3 \le k < 5$ bad behaviour (-);
- $k \ge 5$ very bad behaviour (--).

	Northbound runs				Southbound runs			
Regenerative coasting %	G 1	G 2	G 3	G 4	G 1	G 2	G 3	G 4
0	- -	-	+	+	- -	-	+	-
10%	+	+	+	-	+	+	+	- -
20%	+	+	+	-	++	+	+	-
30%	+	+	+	+	++	+	+	+
40%	++	+	+	++	++	+	+	++

Table 1: Quality of vibrations on gearboxes based on kurtosis

The four gearboxes proved to be in initially very different conditions, showing RMS values quite depending on the speed and direction. As an example, Figure 33 and Figure 34 show the application of a 40% regenerative coasting to the worst gearbox in the set (G4). While RMS levels increase, kurtosis value decrease dramatically, confirming that the solution is valid. If the reader is concerned about the quite high value of the regenerative coasting used, he should look at gearboxes G1, G2 and G3: values of 10% of regenerative coasting are generally sufficient to prevent spikes on initially good gearboxes. Regenerative coasting can certainly fix problems of highly defective gearboxes, but its best use is as a prevention measure to be applied to gearboxes since the beginning of their life, when they are certainly in good conditions.

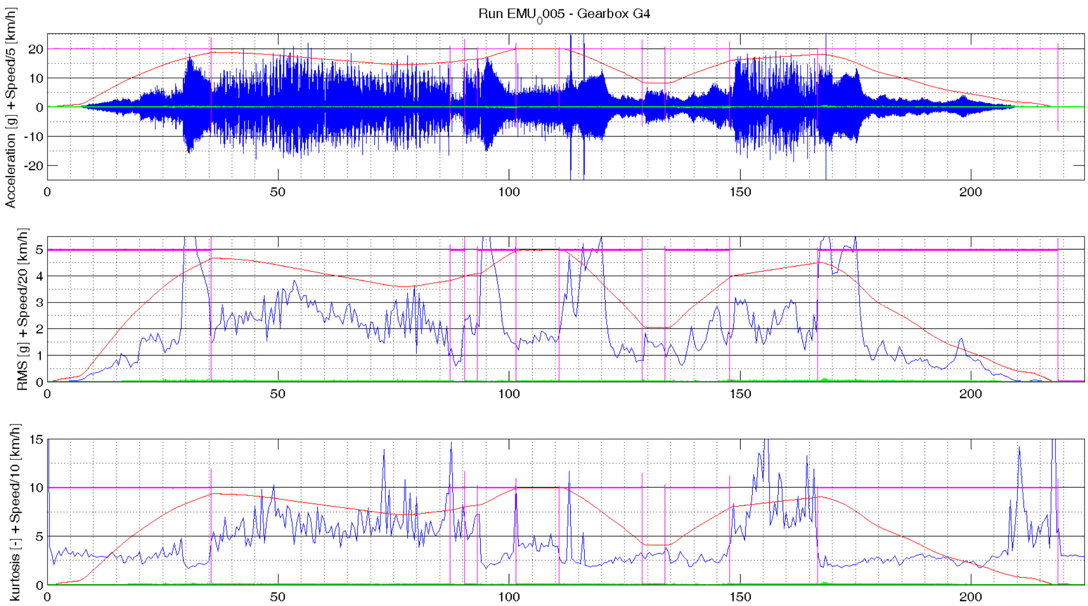

Figure 33: Gearbox 4 with no regenerative coasting (original traction software). Vertical gearbox acceleration (top), RMS value (mid), kurtosis (bottom). Speed and coasting signals are also indicated

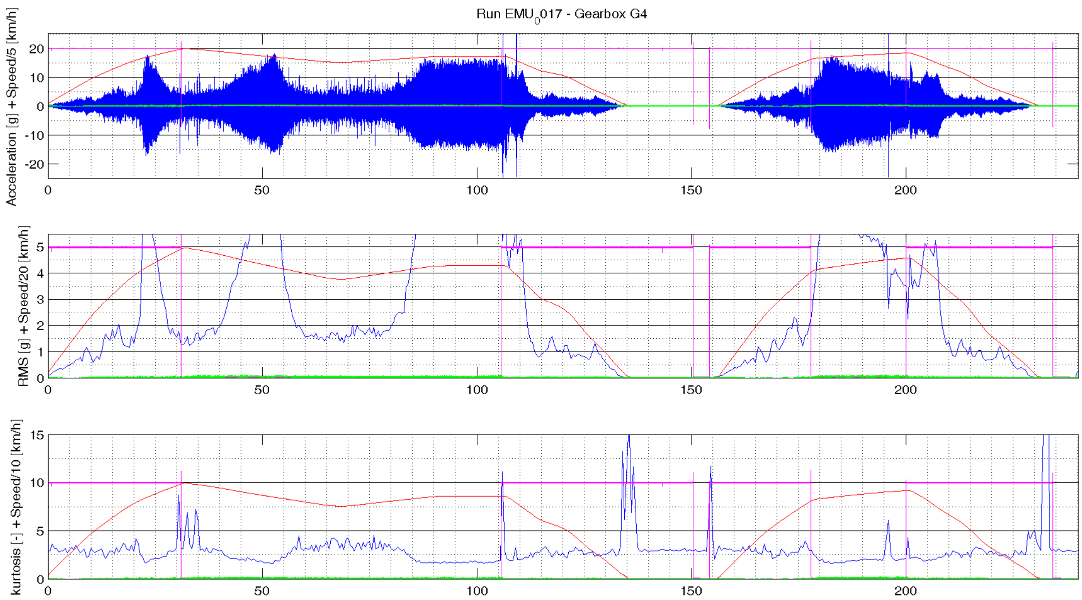

Figure 34: Gearbox 4 with 40% regenerative coasting (modified traction software). Vertical gearbox acceleration (top), RMS value (mid), kurtosis (bottom). Speed and coasting signals are also indicated

8 Conclusions and further developments

Premature failures in a taper bearing of a railway gearbox triggered a set of activities in order to fix the problem. Troubleshooting was particularly difficult as only a limited number of experimental activities were possible without substantial modifications on the gearboxes in service. The root cause of the problem was identified in the high percentage of coasting at high speed run by the trains.

Starting from an existing set of measurements, the authors performed several analyses and designed several retrofit systems capable to remove play, add stiffness and add damping to the various elements of the kinematic chain. Although the majority of these attempts failed, it is believed that the reader can get some useful information in case similar problems are found in this or in other fields of engineering, although the use of lightly loaded (or completely unloaded) transmissions may be not very common outside railway applications.

The final measure applied, i.e. a torque preload by means of the so-called "regenerative coasting" procedure, completely removed the oscillations ("spikes") that are believed to be the root cause of the failures. A companion paper explains the signal processing procedure that allowed to qualify and to accept the proposed measure as a valid criterion to be applied extensively.

The final application policy on the trains that were affected by the problem is ongoing and should be finished by the first months of 2014. The key factors which will drive the definition of the regenerative coasting percentage selected will be the line quality, the initial conditions of the gearboxes and the extent to which software can be modified. A different regenerative coasting strategy could lead for example to much better results, as shown in Figure 35.

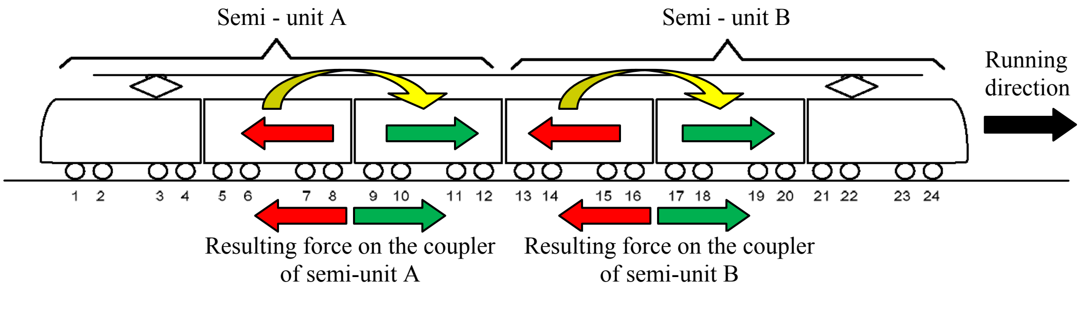

Figure 35: Different regenerative coasting implementation which eliminates the force on the central coupler resulting in lower forces on internal coupler of each semi unit. No power recirculation through the overhead line is needed and the semi units are completely independent

Hopefully the conclusions will be reported at *The Second International Conference on Railway Technology: Research, Development and Maintenance*, 8-11 April 2014, Ajaccio, Corsica, France.

References

[1] A. Bracciali, F. Piccioli, “Effect of load on vibrations of a railway gearbox”, Railways 2014 - The Second International Conference on Railway Technology: Research, Development and Maintenance. Ajaccio, Corsica, France, 8-11 April 2014